Citation
Li, Z. and Chen, W. and Hao, H. 2019. Functionally graded truncated square pyramid folded structures with foam filler under dynamic crushing. Composites Part B: Engineering. 177: ARTN 107410.
http://doi.org/10.1016/j.compositesb.2019.107410

Functionally graded truncated square pyramid folded structures with foam filler under dynamic crushing

Zhejian Li, Wensu Chen*, Hong Hao*

Centre for Infrastructural Monitoring and Protection,

School of Civil and Mechanical Engineering, Curtin University, Australia

*corresponding author: wensu.chen@curtin.edu.au; hong.hao@curtin.edu.au

Abstract

Dynamic crushing responses and energy absorption of functionally graded folded structure with foam fillers are investigated in this study. The proposed structure consists of multiple layers of folded truncated square pyramid (TSP) foldcore with foam fillers added inside each unit cells and the interlayer plates to separate each layer of foldcore and its foam filler. The foldcores are folded using pre-patterned thin aluminium sheets. Two types of foam including cubic shape expanded polystyrene (EPS) foam fillers with density of 13.5, 19 and 28 kg/m^3 and rigid polyurethane (PU) foam with two shapes. Two sets of functionally graded multi-layer structures are achieved by varying the densities of EPS foam fillers (positively/negatively graded EPS) and varying the shapes of PU foam fillers (positively/negatively graded PU) inside each layer of TSP foldcore. These specimens are then crushed under 1 and 10 m/s. Under 1 m/s crushing, excellent crushing responses as energy absorber are observed for both negatively graded and positively graded multi-layer structures with low initial peak force and low fluctuation in resistance throughout deformation. Under 10 m/s crushing, however, positively graded structures show much more uniform load-displacement response with significantly reduced peak crushing force, increased energy absorption than negatively graded structures. Up to 60% increase in specific energy absorption is shown for folded structure with positively graded PU foam as comparing to the uniform structure without foam filler under 10 m/s crushing.

Keywords: functionally graded; dynamic crushing; folded structure; energy absorption

1 Introduction

Sandwich structures have been widely used due to the characteristics such as high specific strength to weight ratio, light weight and high energy absorption capacity [1-3]. Sandwich panel, as its name would suggest, often consists of a cellular crushable core sandwiched by two high strength skins. Under static and dynamic loading, the crushable core is able to undergo large plastic deformation and dissipate a large amount of energy. The cores with different topologies including metallic foam [4, 5], polymeric foam [6], eggbox [7, 8], honeycomb [9], lattice [10], corrugated [11, 12] and load-self-cancelling [13] have been extensively studied under static and dynamic loads such as blast and impact. Many studies suggest that under dynamic loading, conventional honeycomb [14], corrugated [15, 16] and lattice [10, 17] sandwich structures have an inconsistent crushing behaviour with a sudden rise in initial peak crushing resistance and fluctuation in resistance during crushing, which may not be ideal for the application as energy absorption under higher loading rate [1]. Metallic and polymeric foams have uniform deformation process with long plateau stage of consistent crushing resistance. However, most of the stochastic foams have bending dominated deformation [18], which results in a lower crushing resistance than stretching dominated cellular structures of the same density [19].

As a new structural form, folded structures inspired by the art of origami, were introduced as core of sandwich structures. Miura-type foldcore, as one of the common folded sandwich core structures, has been widely studied [20, 21]. With advantages such as open-channel design and high strength to weight ratio, it was proposed to be used as sandwich core of airplane fuselage to reduce weight and avoid moisture accumulation [22]. Other folded structures including origami-patterned vehicle crash box [23], curved crease foldcores [24] and self-locking origami structure [25] have been developed to achieve certain mechanical properties. Truncated square pyramid (TSP) folded structures were proposed and studied both numerically and experimentally under static and dynamic crushing [26, 27]. Due to its unique geometry, ideal structural response was demonstrated with uniform load-displacement response during crushing deformation, and low sensitivity to loading rate. Good energy absorption performance was also shown where its specific energy absorption almost doubled some current energy absorbers made of similar materials with similar densities [7]. Foam filled multi-layer TSP foldcore was also verified by dynamic tests where significant enhancement in energy absorption was demonstrated without inducing a sudden rise in initial peak force [28].

Functionally graded materials (FGM), where the material properties vary layer-by-layer or gradually within the material, are used as cores for sandwich structures. The varying material properties can be achieved by changing cell size, geometrical dimensions [29], wall thickness [30] and density [31, 32]. Many stepwise and continuously graded structures including corrugated [33], honeycomb [34, 35], foams [36], stacked Miura-type foldcore [37] and lattice [38, 39] were investigated recently. Improved energy absorption and crushing behaviour are shown for functionally graded structures than their uniform counterpart under impact or blast loading. It is worth noting that many existing graded structures are permanently bonded between layers and some complex graded structures such as lattice structures can only be manufactured by additive manufacturing [38, 39], which limits the size of the structure and can be costly.

In this study, three-layer TSP folded structure with different foam fillers is explored to achieve a layer-by-layer functionally graded sandwich structure. Two sets of foam fillers are used. For the first set, three different densities of cubic expanded polystyrene (EPS) foam fillers are inserted into three layers of foldcore. For the second set, shaped and cubic rigid polyurethane (PU) foam fillers are inserted into two layers with no foam filler added on the third layer. Two different foam filling orders including positively and negatively graded are considered for both sets of EPS and PU foam. These foams filled graded multi-layer TSP structures along with the uniform TSP structure without filler are then tested under different impacting speeds. Crushing response and energy absorption are then compared among these different set-ups.

2 Layer geometry

2.1 Folding geometry of foldcore

In this study, four connected unit cells are used for each layer of the folded structure. The folding pattern and a folded unit cell of TSP structure is shown in Figure 1. The black solid lines are the boundary of each sheet pattern, where the blue and red lines are mountain and valley creases, respectively. Multiple aluminium thin sheets are stacked together and then cut into the designed pattern using water jet cutting machine all at once. Each layer of TSP foldcore is then folded manually according to the designed crease pattern. The designed dimension of each unit cell is 40x40x20 mm, with bottom edge length, *a*, of 40 mm, top edge length, *b*, of 20 mm and height, *H* of 20 mm. The designed slope of TSP foldcore sidewalls is 63 degrees. Each layer, consisting of four connected unit cells, has a designed dimension of 80x80x20 mm. All specimens are folded from Al 1060 sheets with thickness of 0.26 mm. Relative density of each layer of foldcore without foam filler is about 2.7%, which is calculated using the material volume divided by the overall volume of each foldcore. It should be noted that the geometry of the patterns is determined by the given values of *a, b* and *H*.

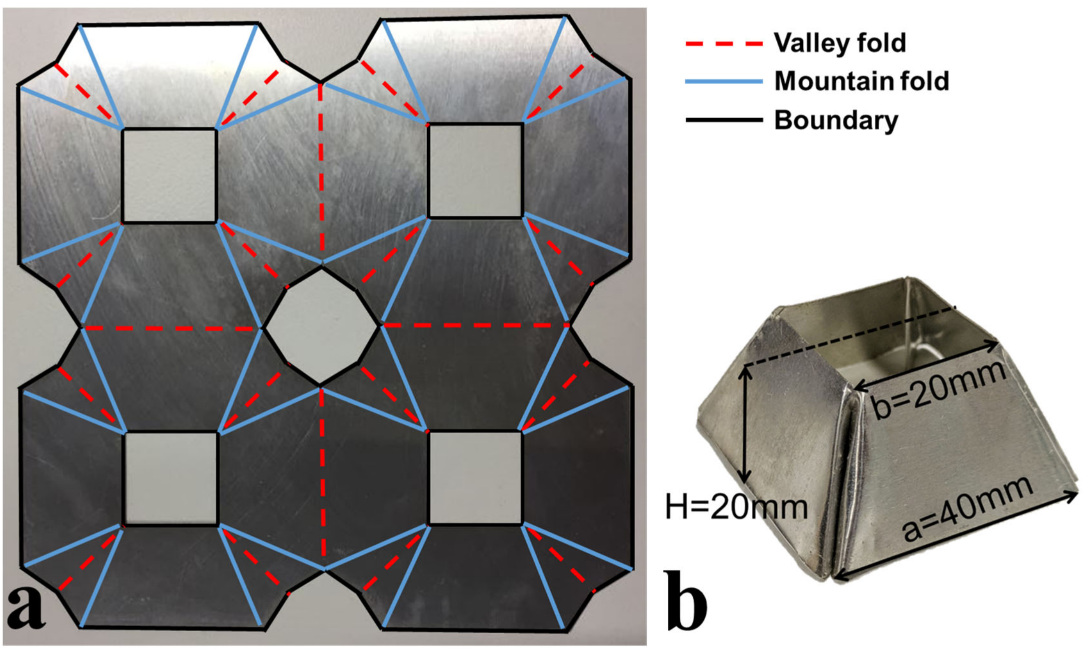

Figure 1. (a) Waterjet cutting pattern and folding crease of a four-unit TSP foldcore; (b) a folded unit cell of TSP foldcore

All testing specimens are prepared by hand folding the patterned aluminium sheets. Imperfections cannot be avoided in this process on the bent sidewalls with uneven levelling for unit cells on the same layer, which results in the gaps between foldcore and supporting plate, as well as uneven initial contact of top edges of foldcore to crushing head. The measured height of foldcore specimens varies between 21 to 23 mm, slightly larger than the designed height of 20 mm. These imperfections could lead to reduction in initial stiffness of the proposed TSP foldcore while the overall crushing response and energy absorption are barely affected. As shown in Figure 2, 3D Direct Image Correlation (3D DIC) analysis is carried out to evaluate the surface flatness of the sidewalls of folded specimens. The maximum difference on the sidewall is about 0.765 mm (-0.485 mm to 0.28 mm) over the length of 40 mm of the bottom edge, as shown in the scale legend in Figure 2. Some imperfections such as bending, or torsion may still exist on triangular interconnections between sidewalls and around the crease lines. Overall, the finishing of the TSP foldcore specimens is acceptable. It should be noted this manufacturing error is also observed even in some of machine pressed Miura-type foldcores in previous studies by other researchers [40], and cannot be completely eliminated. Such errors can be reduced by more advanced machine folding.

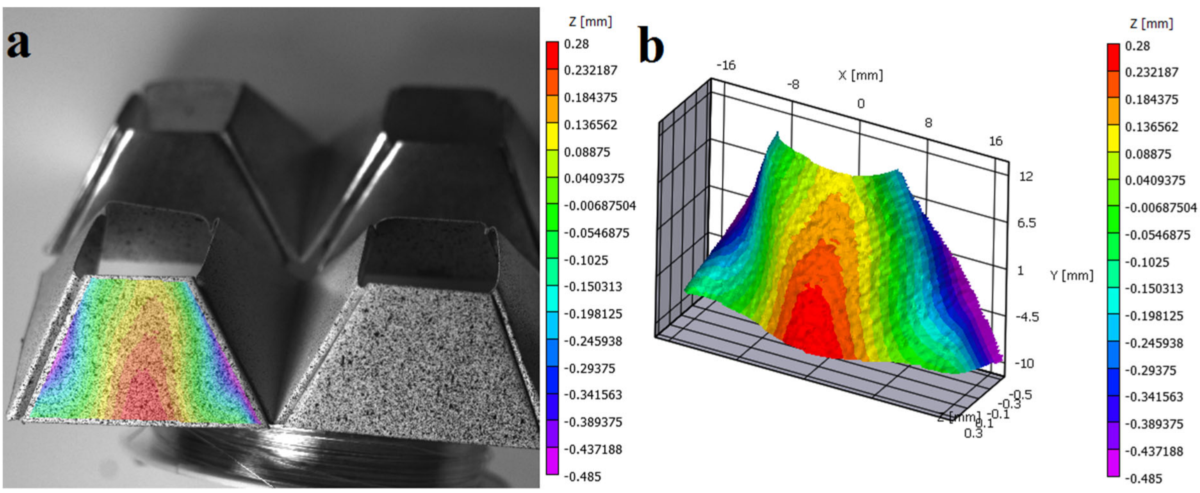

Figure 2. (a) Surface flatness analysis of one sidewall of TSP foldcore using 3D direct image correlation (DIC); (b) sidewall model reconstruction

2.2 Foam filler configurations and multi-layer set-up

Table 1. Five graded configurations and total weight of the foldcore

Notation	**Graded order**	**Foam filler (kg/m^3)**			**Total mass (g)**
		Top layer	Middle layer	Bottom layer	
3TSP	Uniform	-	-	-	28.1
3TSP-EPS-C-PG	Positively graded (PG)	Cubic EPS13.5	Cubic EPS19	Cubic EPS28	29.6
3TSP-EPS-C-NG	Negatively graded (NG)	Cubic EPS28	Cubic EPS19	Cubic EPS13.5	29.6
3TSP-PU-PG	Positively graded (PG)	-	Cubic PU35	Shaped PU35	30.9
3TSP-PU-NG	Negatively graded (NG)	Shaped PU35	Cubic PU35	-	30.9

Five different graded configurations are listed in Table 1. These include a uniform multi-layer folded structure without filler, two sets of negatively and positively graded multi-layer folded structures achieved by varying foam filler densities and shapes. A total of five different types of foam fillers are inserted into the foldcores: cubic expanded polystyrene (EPS) with densities of 13.5, 19 and 28 kg/m^3, cubic and shaped rigid polyurethane (PU) foam with density of 35 kg/m^3. The densities of foam filled TSP core range between 75 and 88 kg/m^3, where a TSP foldcore without foam filler has a density of 73 kg/m^3 (2.7% relative density). Based on previous investigation of multi-layer folded structure with uniform foam fillers, the crushing resistance of the foam filled structure is proportional to the foam strength and the support provided from foam to the foldcore. The positively graded structure is defined as increasing density and crushing strength from top to bottom layer. The notations of these structures are listed in Table 1. For instance, 3TSP-EPS-C-NG represents three-layer truncated square pyramid structure filled with negatively graded cubic EPS foam fillers from the top to the bottom layer.

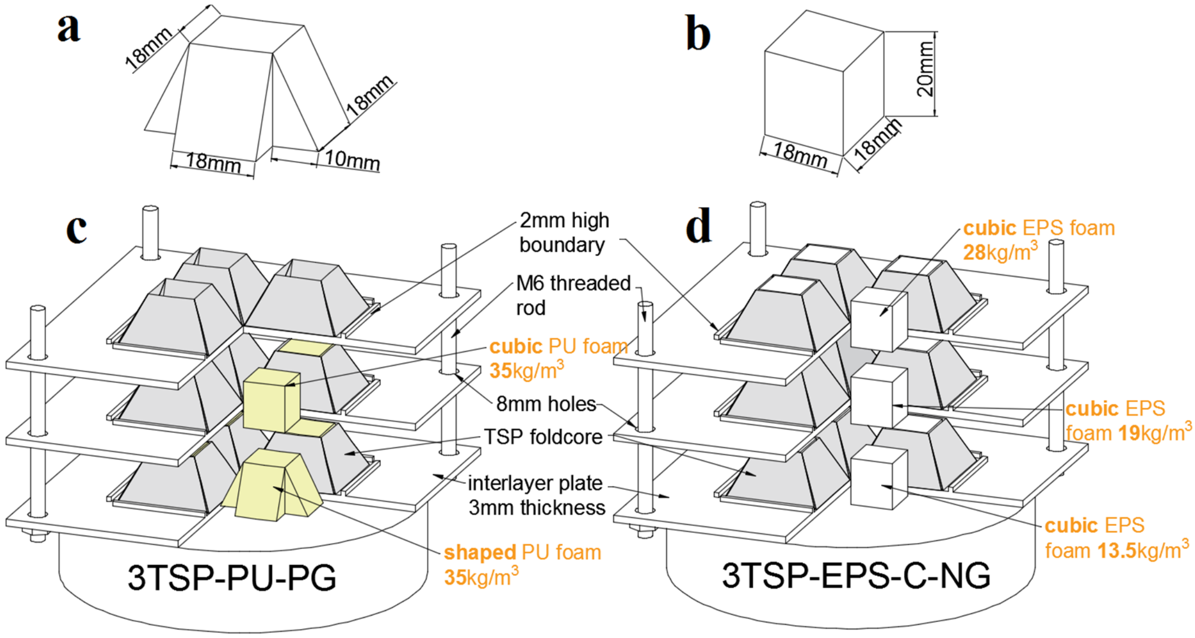

Figure 3. (a) Dimension of shaped foam filler; (b) dimension of cubic foam filler; (c) multi-layer set-up of PU foam filled positively graded folded structure; (d) cubic EPS foam filled negatively graded folded structure; Note: quarter of the plates and foldcores are cut out to illustrate the added foam fillers

The geometry of these two shapes of foam filler and the graded multi-layer set-up are shown in Figure 3. Four units of foam filler are inserted into each layer of foldcore, achieving graded effect on different layers. Each layer of foldcore and foam filler is separated by interlayer plate made of Al 5083 with thickness of 3 mm. To constrain the in-plane movements of foldcore sidewalls, 2 mm high boundary curbs are also included on the interlayer plates along the four sides. Thread rods are bolted onto base plate and function as guide for interlayer plates to move in the vertical direction. The holes located at four corners of the plates have diameter of 8 mm, sufficiently larger than the M6 threaded rods of 6 mm diameter. Unlike the common sandwich structure designs, where the skins and core are often permanently bonded [15, 20], each layer of the proposed graded folded sandwich structure is simply supported. After impact, each layer of deformed core can be easily removed and replaced by a new core structure. Only one set of plates are used for all different graded configurations throughout the impact tests in this study. No noticeable plastic deformation is observed on any plate after dozens of impact tests.

2.3 Material properties

The TSP cores are folded from Aluminium 1060 thin sheet with thickness of 0.26 mm which gives a relative density of 2.7% for all foldcores. Aluminium 1060 has a minimum 99.6% of aluminium content [41]. The measured mechanical properties are listed in Table 2, and the true stress-strain curve is measured in the previous study [42]. The interlayer plates and base plate are made of Al 5083 alloy, material properties are listed in Table 2. As plates made of Al 5083 is much thicker and of higher yield stress than TSP foldcore made of Al 1060, no noticeable plastic deformation of the plates is observed throughout the impact tests.

Table 2. Mechanical properties of aluminium 1060 and 5083 [43]

Parameter	Young's modulus (GPa)	Poisson's ratio	Yield stress (MPa)	Density (kg/m^3)
Aluminium 1060 [42]	69	0.33	66.7	2710
Aluminium 5083 [43]	71	0.33	215.0	2660

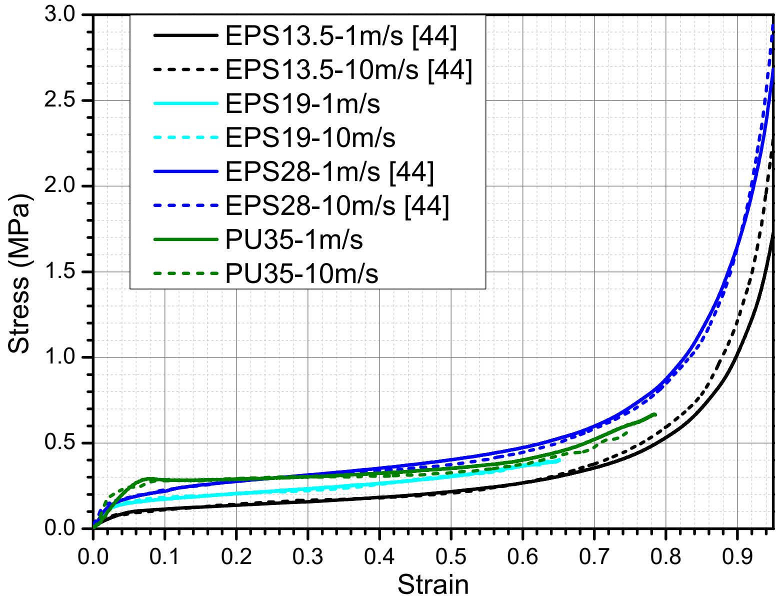

Figure 4. Engineering stress-strain curves of EPS13.5 [44], EPS19, EPS 28 [44] and PU35 under 1 m/s and 10 m/s crushing speed

Uniaxial compressive tests are carried out for EPS19 and PU35 foam material under the same crushing rate (1 and 10 m/s). Stress-strain data for EPS13.5 and 28 are obtained from the previous study [44]. Engineering stress-strain curves of these foam materials under two loading rates are shown in Figure 4. The foam specimens have a diameter of 75 mm and height of 50 mm. Multiple tests are carried out for each loading scenario. Same testing equipment is used to test the graded structures. Two crushing speeds on the foam materials are used for the proposed graded structures as well. The labelled crushing speed is not necessarily the actual moving speed of the impact head throughout the crushing, due to the deceleration at later stage. Details of the testing machine and crushing speed are provided in section 3.

3 Test set-up

3.1 Dynamic test

Instron VHS 160/100-20 high speed testing machine is used for dynamic crushing tests of these graded multi-layer folded structures. Fastcam APX RS high speed camera is used for recording with the frame rate between 2,000 and 5,000 fps depending on the crushing speed of the tests. The impacting head and base support are discs with diameter of 100 mm, smaller than the distance between the rods. Each layer of foam filled foldcore has a height of 20 mm, and the interlayer plate is 3 mm thick. For three-layer graded structures, the actual overall height varies between 71 and 74 mm instead of the designed 69 mm height. As previously discussed, the hand folding process induces imperfections and causes slight uneven levelling between unit cells within a layer. This, however, has negligible effect on overall crushing response of the graded structure including energy absorption and peak crushing force, although slight reduction of initial stiffness is observed. A total of 24 tests are carried out. Two to three specimens are tested for each loading and graded scenario and the load-displacement curve closest to the average is selected to represent the case.

3.2 Crushing speed

Two crushing speeds, i.e. 1 m/s and 10 m/s are considered in this study to compare the crushing responses of the graded structures with the increasing speed under low to intermediate crushing speeds [45]. The testing machine is designed to impact and crush the specimens at a constant speed. However, constant crushing speed cannot be maintained perfectly throughout the entire process. The impacting head requires to be decelerated to zero speed before reaching a pre-set stopping position to avoid impacting the base support disc. Therefore, with the progressing of the crushing, the crushing speed decreases. The actual crushing speeds of the impacting head corresponding to the designated crushing speed of 1 and 10 m/s are not constant throughout the crushing process. Under lower crushing speed of 1 m/s, the distance required for deceleration is shorter, therefore a constant crushing speed can be achieved for the most portion of the deformation. However, longer deceleration distance is required under higher crushing speed of 10 m/s, which leads to decreasing crushing speed. In this study, the crushing speed (i.e. 1, 10 m/s) refers to the speed setting for the test instead of the actual crushing speed which is not a constant value throughout the crushing process in the test.

4 Results and discussions

4.1 Low-speed impact (1m/s)

4.1.1 Damage mode comparison (quasi-static and 1 m/s crushing)

Deformations of the crushing of three-layer TSP folded structure without foam fillers (three cores and three plates) are shown in Figure 5 for quasi-static and 1 m/s crushing cases. The loading rate of 2 mm/min is applied for the structure under quasi-static crushing. Obvious difference in deformation can be observed between these two loading cases. Simultaneous deformations across all three layers are shown for the quasi-static crushing case. This simultaneous deformation results in a smoother load-displacement response of the structure which is shown in section 4.1.2. Furthermore, the interlayer plates are tilted for quasi-static condition, and this is caused by the difference in crushing strength of the unit cells on the same layer. Due to the very low loading rate (2 mm/min), even slight difference in crushing strength of unit cells can cause plate tilting and uneven loading to the next layer. Under 1 m/s crushing, the interlayer plates are less tilted and the layer-by-layer deformation is shown in Figure 5 (b, d). Under 1 m/s impact loading, the foldcore has less time to deform along the weaker portion of the unit cells as compared to quasi-static crushing, especially during the initial impacting stage. Therefore, foldcore within a same layer is more evenly crushed among unit cells, resulting in less tilting interlayer plates.

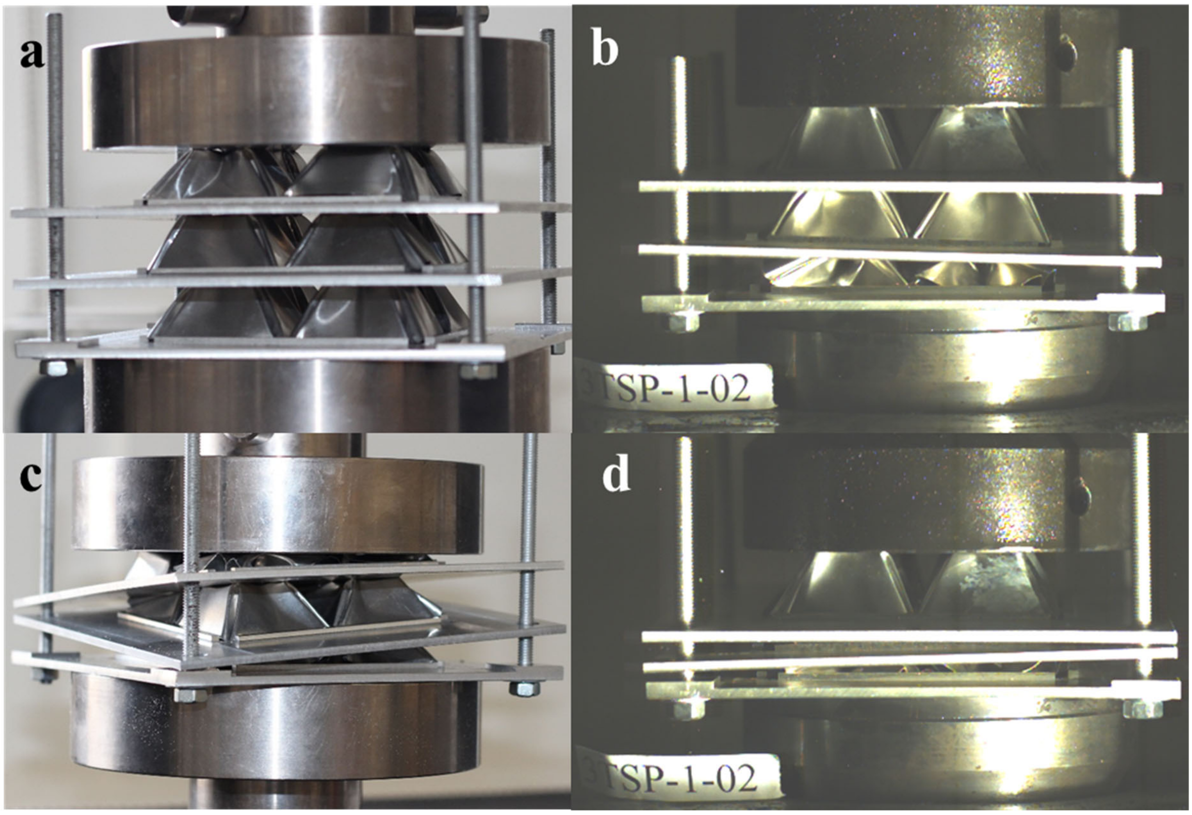

Figure 5. Deformation of three-layer TSP folded structure without foam fillers (a) early stage of quasi-static (2 mm/min) crushing; (b) early stage of 1 m/s crushing; (c) later stage of quasi-static crushing; (d) later stage of 1 m/s crushing

In addition, it is observed that only the bottom layer undergoes large deformation while the other two layers almost remain their original shapes at the early stage. The deformation then propagates to the mid and finally to the top layer. The initiation of the layer-by-layer crushing from the bottom layer is caused by stress wave interferences under impact condition [46, 47]. Under the impact of 1 m/s, the stress at top layer is not high enough to cause layer deformation at the moment of impact, thus the stress wave propagates downwards. When the reflected wave from the stationary base meets with the propagating stress wave from the impact end, the superimposed stress exceeds the layer buckling stress and thus the damage occurs near the base end. Under higher speed impact, the stress at the impact end might exceed the buckling stress of the structure, the damage occurs at the impact end rather than the base end. As reported in the previous study, the damage initiates from the top layer under 15 m/s impact.

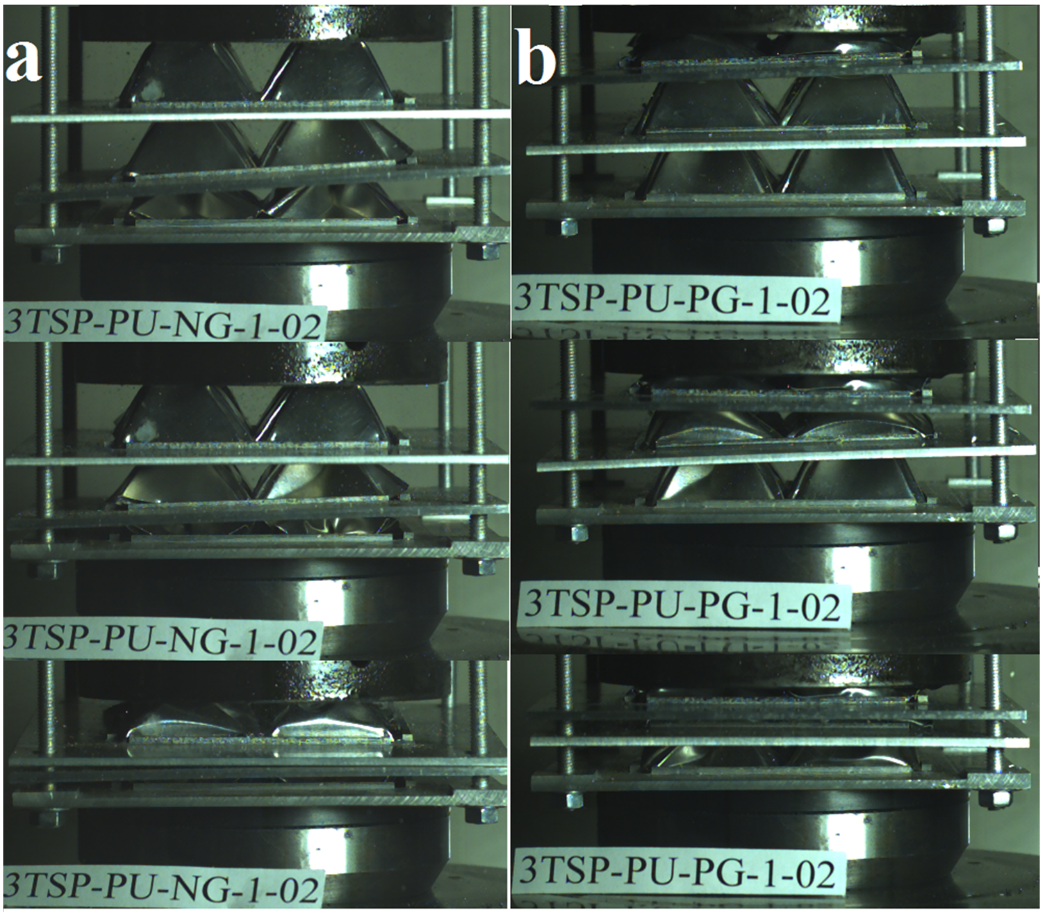

Figure 6. Deformation of (a) negatively; (b) positively graded structures with PU foam filler under 1 m/s crushing

Crushing process of the NG and PG folded structure with PU foam fillers under crushing rate of 1 m/s is shown in Figure 6. The last two digit in the label is the specimen number. For instance, 3TSP-PU-NG-1-02 stands for the second test of 3-layer TSP folded structure with negatively graded PU foam fillers from top to bottom. This also shows a layer-by-layer crushing of the graded structures, similar to the uniform TSP folded structure without foam fillers. However, unlike the structure with uniform foldcores that crushing initiates at the bottom layer as shown in Figure 5 (b), the crushing initiates at the weaker layer of the graded structure, which is the bottom layer for NG structure and the top layer for PG structure. The initiation of the buckling of each layer corresponds to three peaks as shown in section 4.1.2. The differences in load-displacement curves can be found among structures with different graded configurations. Comparing to the uniform TSP folded structure without foam fillers, graded structures have higher local peaks. The foam filler provides not only direct compressive strength to the structure but also the support and interaction to the sidewalls. As previously investigated [48], the interactions become more apparent when sidewalls deform. Since more portions of sidewalls are in contact with the foam fillers to resist sidewall buckling, the crushing resistance of the structure significantly increases.

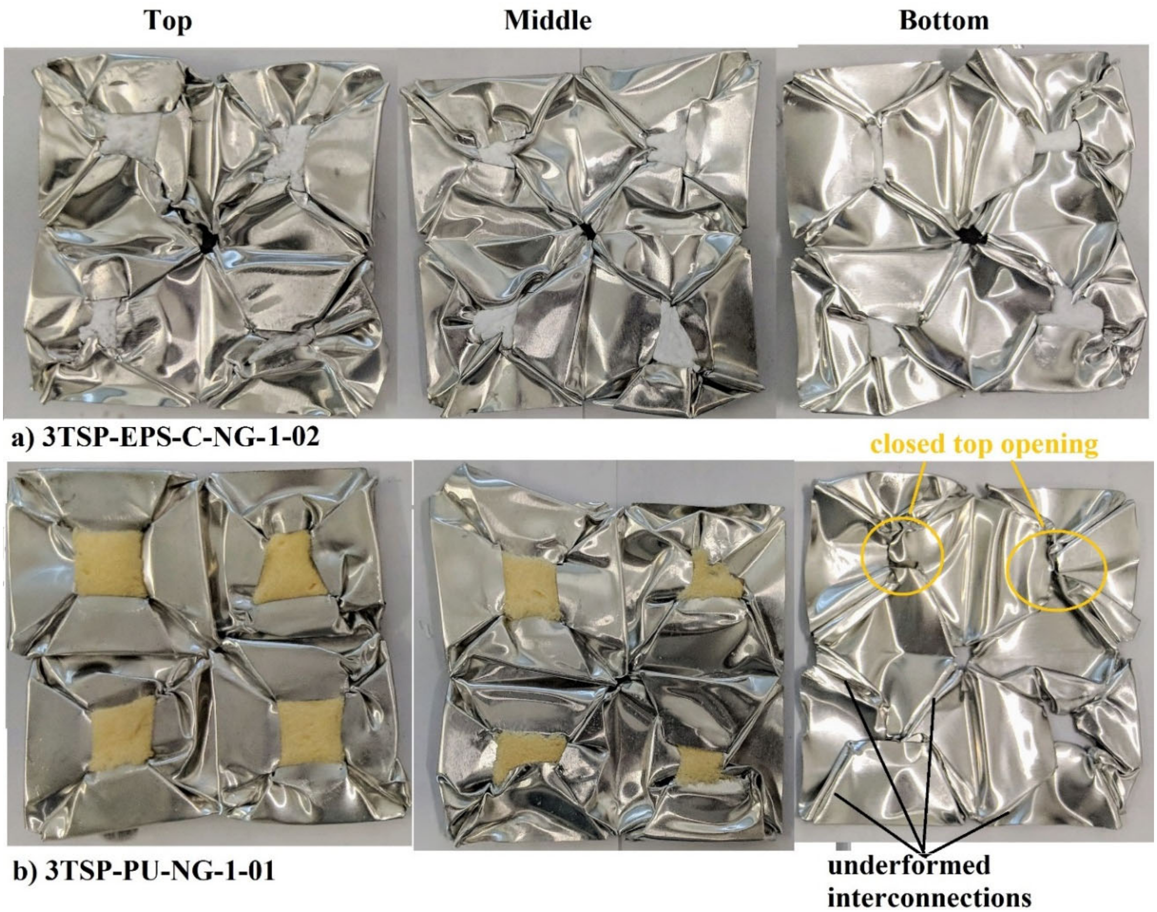

Figure 7. Damage modes of negatively graded structure with (a) cubic EPS foam fillers;(b) PU foam fillers, under 1 m/s crushing

The NG and PG folded structures with EPS foam fillers show similar behaviour to the PU foam filled graded structures. However, the layers of NG and PG structures show opposite crushing order since the crushing of the structure always starts from the weakest layer under low impacting speed. Due to the difference in material properties between EPS and PU foams, three peak values in load-displacement curves are not the same as shown in section 4.1.2. The layer with shaped PU foam filler has the highest peak, as the designed shape (Figure 3 a) better fits the slope of the sidewalls and enhances the interaction between the foam filler and sidewalls. This added shaped foam filler also results in a change of damage mode as compared to the bottom layer where no foam filler is added, as presented in Figure 7 (b). The added shaped foam on the top layer of 3TSP-PU-NG-1-01 provides extra support to the sidewalls during deformation. Therefore, the faces of sidewalls bend outwards horizontally, and the top openings remain their original square shape. For the layer without foam filler or with cubic foam filler (bottom and middle layers), the sidewalls bend inwards, resulting in more deformation on the top openings before deformation. The damage modes on three layers of positively graded PU filled structures are shown in Figure 8 (b). This change of damage mode leads to the highest peak force out of the three peaks in load-displacement curves when the shaped foam filled layer undergoes deformation.

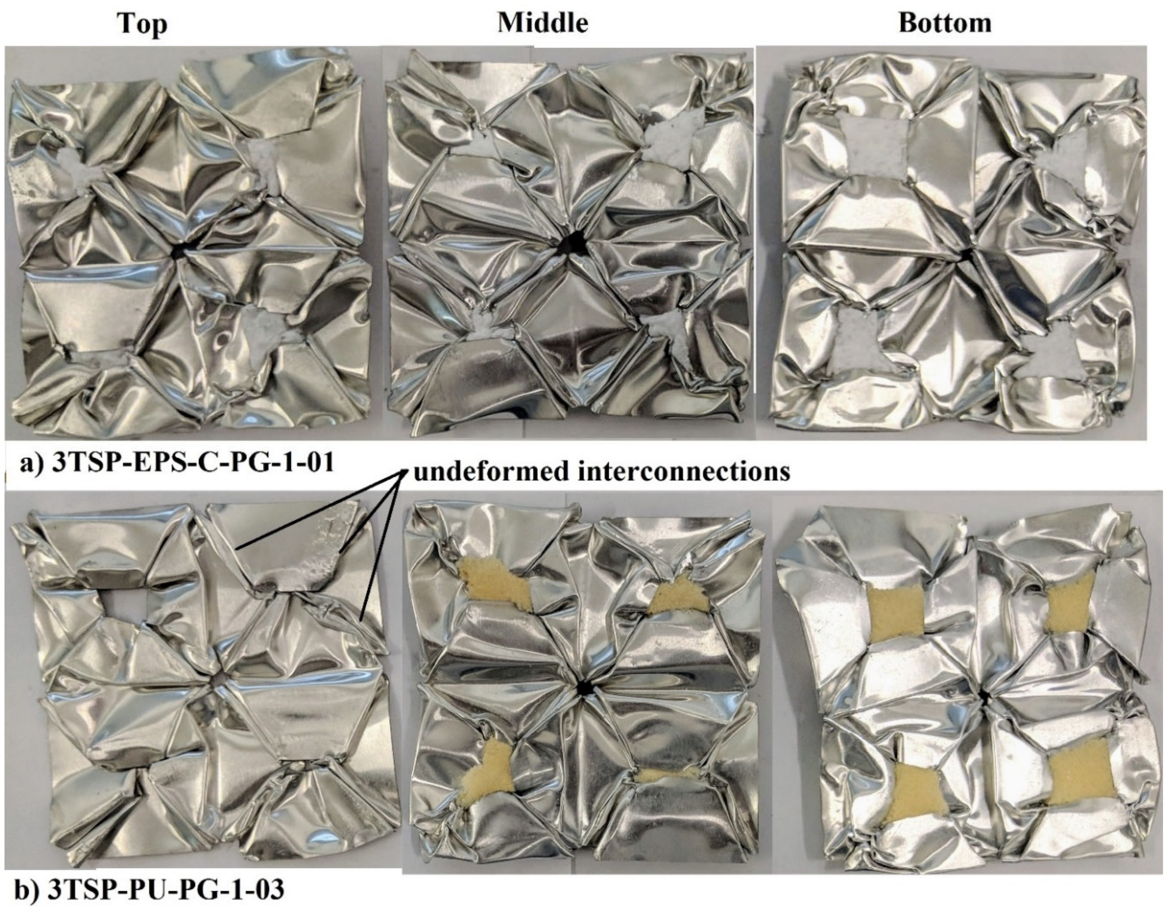

Figure 8. Damage modes of positively graded structure with (a) cubic EPS foam fillers;(b) PU foam fillers, under 1 m/s crushing

4.1.2 Structural response and energy absorption (1 m/s crushing tests)

Structural response and energy absorption are compared in this section. Peak crushing load, P_{peak}, average crushing load, P_{ave}, uniformity ratio, U, densification strain, ε_D, and specific energy absorption (SEA) are selected for evaluation of the crushing response and energy absorption capacities of these different graded structures. The densification strain, ε_D, is calculated by the displacement at the onset of densification divided by the total height of the foldcores. Densification is the stage where crushing resistance rises suddenly due to the compaction of structure. The total height of foldcore in this study is 60 mm which consists of 3 layers of 20 mm high foldcore. Total height does not include the thickness of interlayer plates, as no deformation and energy absorption is presented on these plates. The average crushing force, P_{ave}, is the average crushing resistance of the structure before it reaches densification, and is defined as follows:

$$P_{ave} = \frac{\int_0^{\varepsilon_D} P(\varepsilon) \cdot d\varepsilon}{\varepsilon_D} \qquad (1)$$

where P is the crushing force and ε is the strain, which is calculated by crushed distance over total height of foldcores. The peak crushing force (P_{peak}) is defined as the overall peak force before densification in this study. Uniformity ratio is the ratio between peak and average crushing forces as:

$$U = \frac{P_{peak}}{p_{ave}} \qquad (2)$$

It is worth noting that the peak crushing force is often defined as the initial peak force in many studies [49, 50]. As for conventional sandwich structures such as honeycomb [50], lattice [10] and Miura-type foldcore [20], sudden rise and fall in crushing resistance occurs at initial stage which can be several times larger than its average crushing force. However, for the folded structures considered in the present study, this initial peak force is not necessarily the overall peak force before densification. Therefore, in this study the uniformity ratio is defined by using the overall peak force instead of the initial peak force. The specific energy absorption is defined as

$$SEA = \frac{P_{ave} \cdot \varepsilon_D \cdot H}{m_{TSP} + m_{foam}} \quad (3)$$

where H is the overall height of the foldcores, m_{TSP} and m_{foam} are the overall mass of the TSP foldcore and overall mass of the foam filler, respectively.

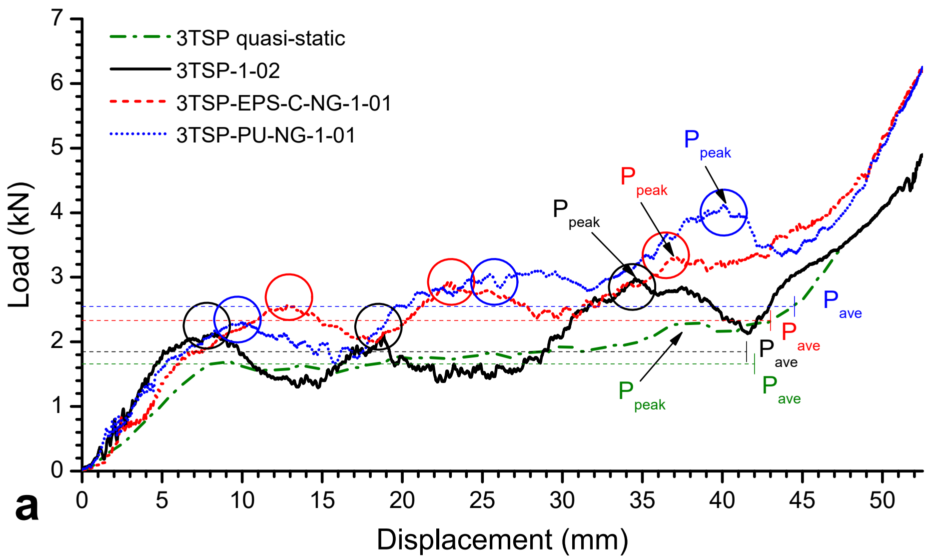

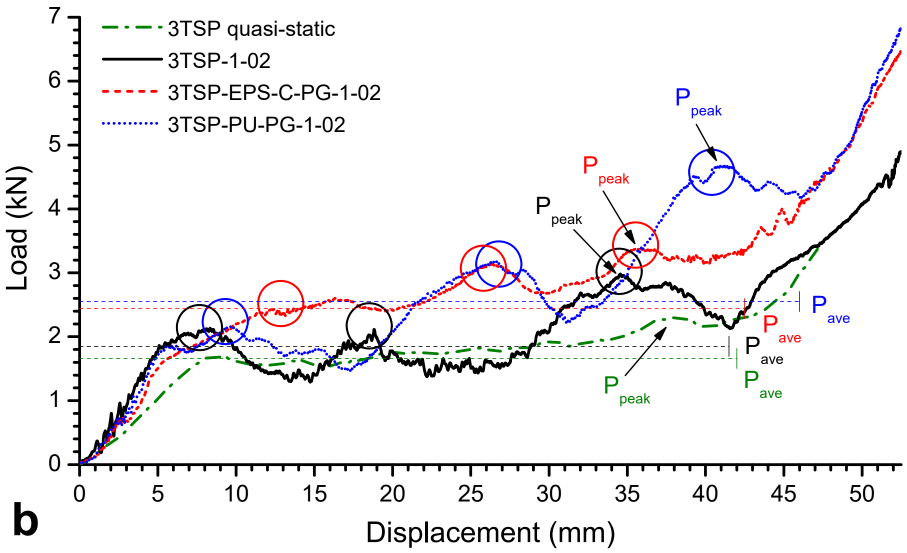

Figure 9. Load-displacement curves of uniform multi-layer TSP folded structure, (a) negatively graded folded structures; (b) positively graded folded structures under 1 m/s crushing; Marked out local peaks corresponds to initiation of buckling of the three layers

The load-displacement curves of multi-layer graded folded structures under 1 m/s crushing are shown in Figure 9. The average crushing forces are also calculated and indicated by the same coloured lines as the curves. The end bar of average force line represents the densification position of the structure where sudden and consistent rise of the crushing force occurs due to the compaction of the structure. The overall crushing response of these structures indicates good performances, with low fluctuations and a long plateau before reaching densification. As previously mentioned, the initial stiffness of structure is slightly lowered due to the imperfections such as uneven levelling and existing gaps between foldcore and plates. This can be observed by the lower slope of curves before 1 to 2 mm displacement. However, this has little effect on energy absorption and overall crushing response of the multi-layer folded structures. It is also clear that the graded structures have a higher average crushing resistance than uniform folded structures without foam filler. As can be noted, the increment in compressive strength of the structure with added foam filler is much greater than the compressive strength of the added foam itself. This great improvement in compressive strength to the folded structure by adding foam filler is due to the interaction effect between foam and the walls [48, 49]. As marked out in circles in Figure 9, three local peaks can be observed for all graded and non-graded folded structures under this crushing speed. These peaks are associated with the initiation of buckling of the sidewalls in each layer. Under quasi-static loading, the load-displacement response is smoother due to simultaneous deformation on all layers. Furthermore, the foam filled graded structures have higher peak resistance than the case without foam fillers due to both added material and foam-sidewall interaction effect.

Structural responses of these graded structures are given in Table 3. The differences in the crushing response parameters of graded structures are minimal under low impacting speed. Both negatively graded and positively graded structures with the same set of foam fillers have similar crushing parameters. For instance, under 1 m/s crushing, negatively and positively graded structures with EPS foam filler show very similar peak, average crushing resistance, uniformity ratio, densification strain and specific energy absorption, although the crushing process is not the same as presented above. Similarly, negatively graded structure with PU foam filler has almost identical crushing parameters as the positively graded structure with PU foam filler. Significant enhancement in average crushing force (25% to 39%) is shown for foam filled graded structure as compared to uniform unfilled structure, while the mass of foam filler only increases between 5 and 10%. Excellent performances in energy absorption are shown for all folded structures with or without foam filler. The SEA varies between 2.50 J/g and 3.80 J/g, which is higher than 0.82-2.51 J/g of typical graded folded structures made of stronger sheet materials and higher core densities (e.g., brass, with Young's modulus 111.1 GPa and yield stress 142 MPa) [37].

Table 3. Crushing responses of different graded structures under 1 m/s crushing speed

Graded configurations	**P_{peak} (kN)**	**P_{ave} (kN)**	**U= P_{peak} /P_{ave}**	**ε_D**	**SEA (J/g)**
3TSP-Quasi-static	2.30	1.66	1.386	0.70	2.50
3TSP-1-02	2.96	1.84	1.598	0.69	2.73
3TSP-EPS-C-NG-1-01	3.30	2.33	1.416	0.72	3.39
3TSP-PU-NG-1-01	4.12	2.55	1.616	0.74	3.67
3TSP-EPS-C-PG-1-02	3.37	2.44	1.381	0.71	3.50
3TSP-PU-PG-1-02	4.68	2.55	1.835	0.76	3.80

Under 1 m/s crushing speed, the graded structures have enhanced average crushing resistance and energy absorption capacity due to the added foam filler. However, difference in positively or negatively graded structure is minimal. For each foam filler configuration considered in the present study, positively graded structures show similar crushing parameters as their negatively graded counterpart. This is due to the layer-by-layer deformation of the structure. Under low crushing speed, the deformation initiates at the weakest layer, followed by the collapsing of the second and then final layer, which are associated with three local peaks in the load-displacement curves as shown in Figure 9. The graded configuration changes the order of layer crushing, but the compressive strength of each corresponded layer is the same. Therefore, the general trends of load-displacement curves between NG and PG under 1 m/s crushing are similar.

4.2 High-speed impact (10 m/s)

4.2.1 Damage mode comparison (10 m/s crushing)

Different from the low crushing speed cases, the graded configurations show significant influence on load-displacement responses under 10 m/s crushing. Figure 10 (a) shows the crushing at the instant when the overall peak force of NG structure occurs at about 22 mm of displacement as shown in section 4.2.2, and Figure 10 (b) is at the same instant when the PG structure with PU foam fillers reaches the peak resistance. The NG structure has a significantly higher peak force than the PG structure with almost a 40% increase. This is because collision between the middle and bottom interlayer plates occurs on NG structure as shown in the figure, which results in higher force.

In this study, the plates are larger than the foldcore, slight tilting may lead to collision on the edge of the plates. However, the primary reason behind the collision of the plates is the fully crushed foldcore layer. For graded structures, the strength difference between layers is amplified with graded structure due to inertia effect and extra stabilization by both the foldcore and the added foam. The weaker layer is crushed quickly and becomes fully compacted. As shown in Figure 10 (a, b), the first deforming layer is completely crushed, resulting the contact between two plates. However, under 1 m/s crushing, the first deforming layer still has residual height for further deformation for both NG and PG structures as shown in Figure 6. The full compaction of the weaker layer leads to large rise in force being transmitted to the next layer. For NG structures, the foldcore of the first crushed layer is fully compacted (bottom layer), therefore, it leads to huge rise in the reaction force, i.e., the force being transmitted to the base where the load cell is located, as shown in section 4.2.2. For PG structures, the fully compacted layer is at the top, and there are two layers below it that can deform to absorb energy. Therefore, the force transmitted to the base is still relatively small. Similar significant increase in transmitted force due to fully compacted layer subjected to dynamic loading were also reported in the previous analytical and experimental studies [51, 52].

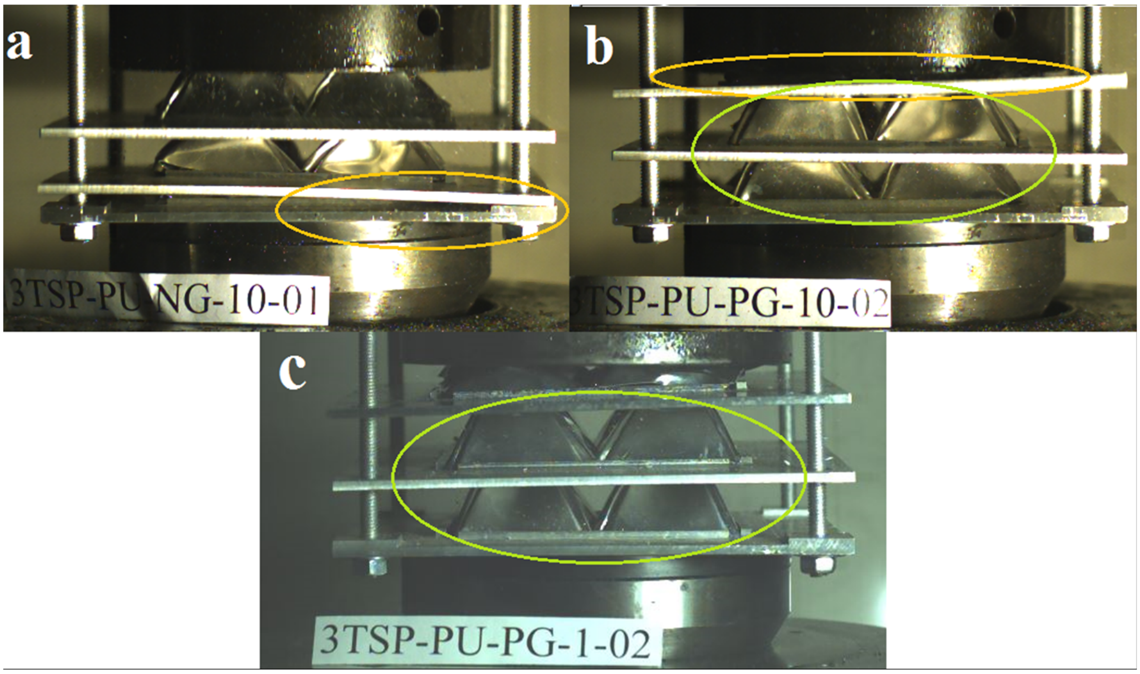

Figure 10. Early deformation comparison of PU foam filled folded structure (a) negatively graded under 10 m/s crushing; (b) positively graded under 10 m/s crushing; (c) positively graded under 1 m/s crushing

Prior to layer-by-layer buckling, all three layers undergo slight deformation simultaneously under high speed crushing, which is slightly different from that under low speed crushing. As can be observed, there is almost no deformation on the middle and bottom layers when the top layer is fully crushed under 1 m/s impact as shown in Figure 10 (c). Under 10 m/s crushing, as shown in green circle in Figure 10 (b), both middle and bottom layers experience some slight deformation when the top layer is fully crushed. This leads to an increased crushing resistance at initial stage due to simultaneous buckling initiation on all layers prior to layer-by-layer deformation. However, the crushing force at later stage is slightly reduced as compared to 1 m/s impacting case, as shown in Figure 16 of section 4.2.2, which is due to the slightly deformed sidewalls of foldcores on middle and bottom layers prior to layer-by-layer crushing.

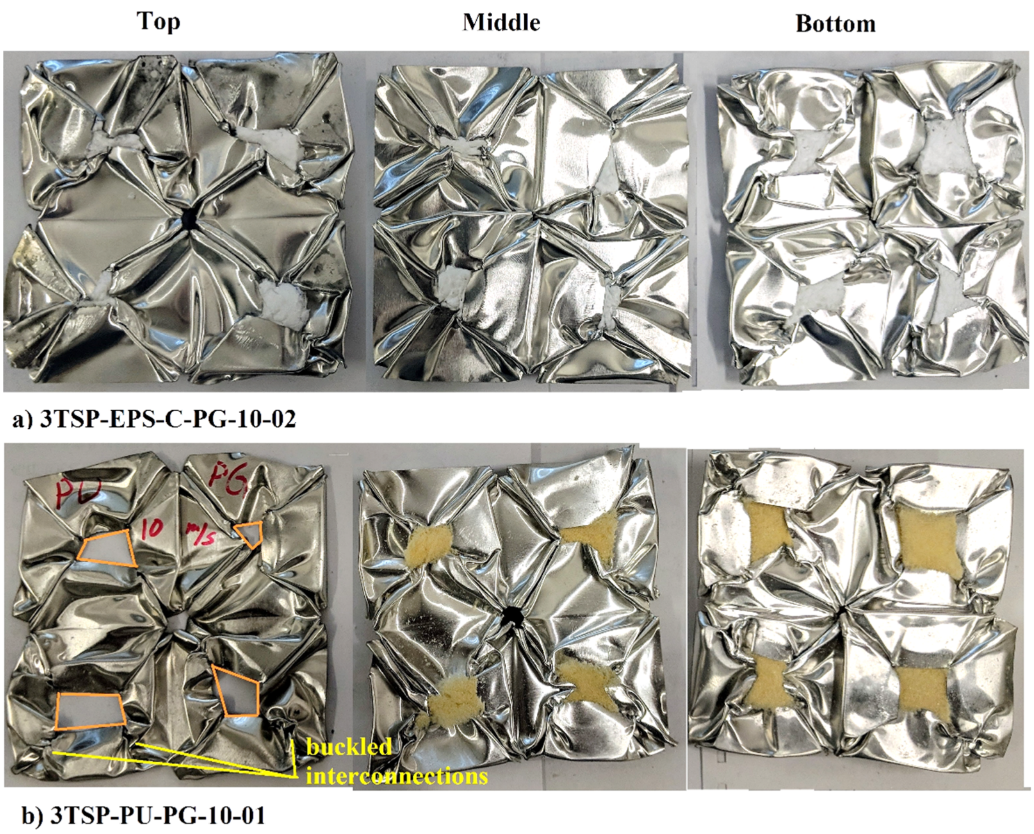

Figure 11. Damage modes of positively graded structure with (a) cubic EPS foam fillers; (b) PU foam fillers under 10 m/s crushing

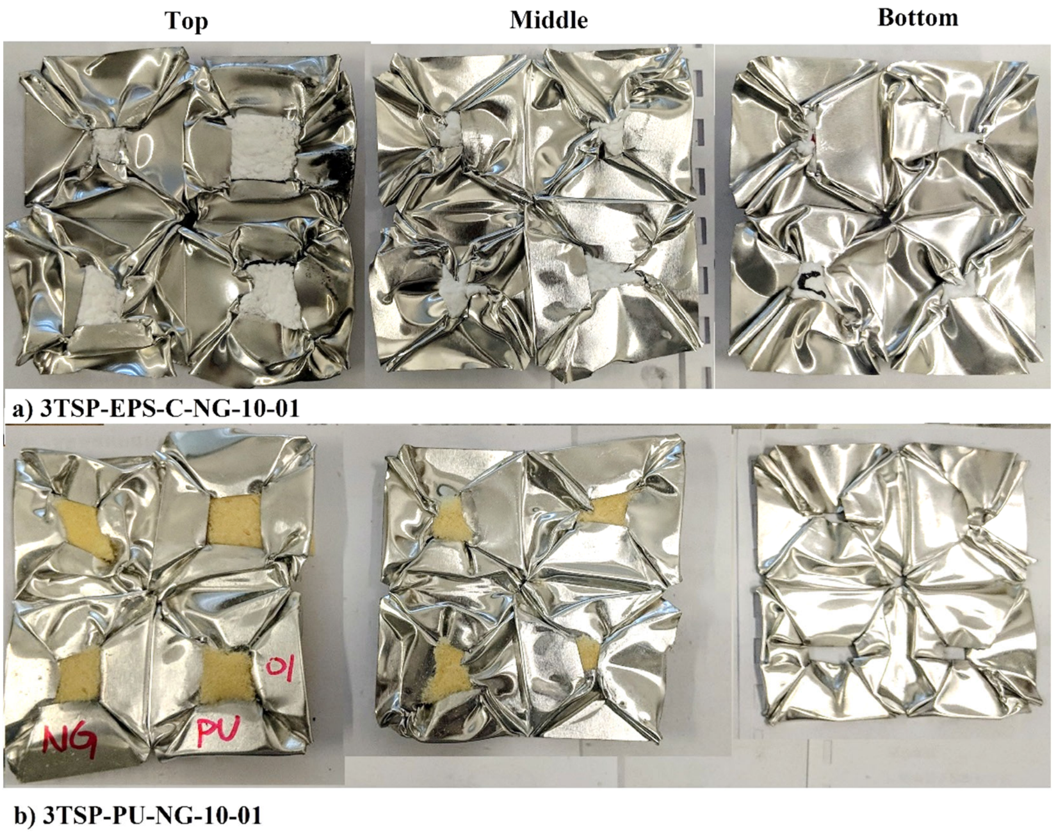

Figure 12. Damage modes of positively graded structure with (a) cubic EPS foam fillers; (b) PU foam fillers under 10 m/s crushing

Damage modes of the two graded structures under 10 m/s crushing are show in Figure 11 and Figure 12. Similar damage modes are observed for foam filled layers due to foam-sidewall interactions. Comparing with 1 m/s crushing (Figure 8 b), larger residual opening and more buckled interconnections on the top layer (i.e. no foam filler) of 3TSP-PU-PG are observed under 10 m/s crushing as shown in Figure 11 (b). This is due to the inertia effect and the geometry of the foldcore causing top portion of the foldcore to deform before the lower portion. As each corner of folded structure consists of two triangular interconnections which strengthen the structure, the foldcore corners rotate about the base instead of buckling under low crushing speed. Under high crushing speed, the deformation of top layer is localized on the top edges of the sidewall. In this case, the top edges roll towards cell centre and the interconnections buckle instead of rotating. Therefore, the interconnection lines are no longer straight as observed under low speed crushing (marked out in Figure 8 (b) top layer), and the top openings are not closed as marked out on the top layer of Figure 11 (b).

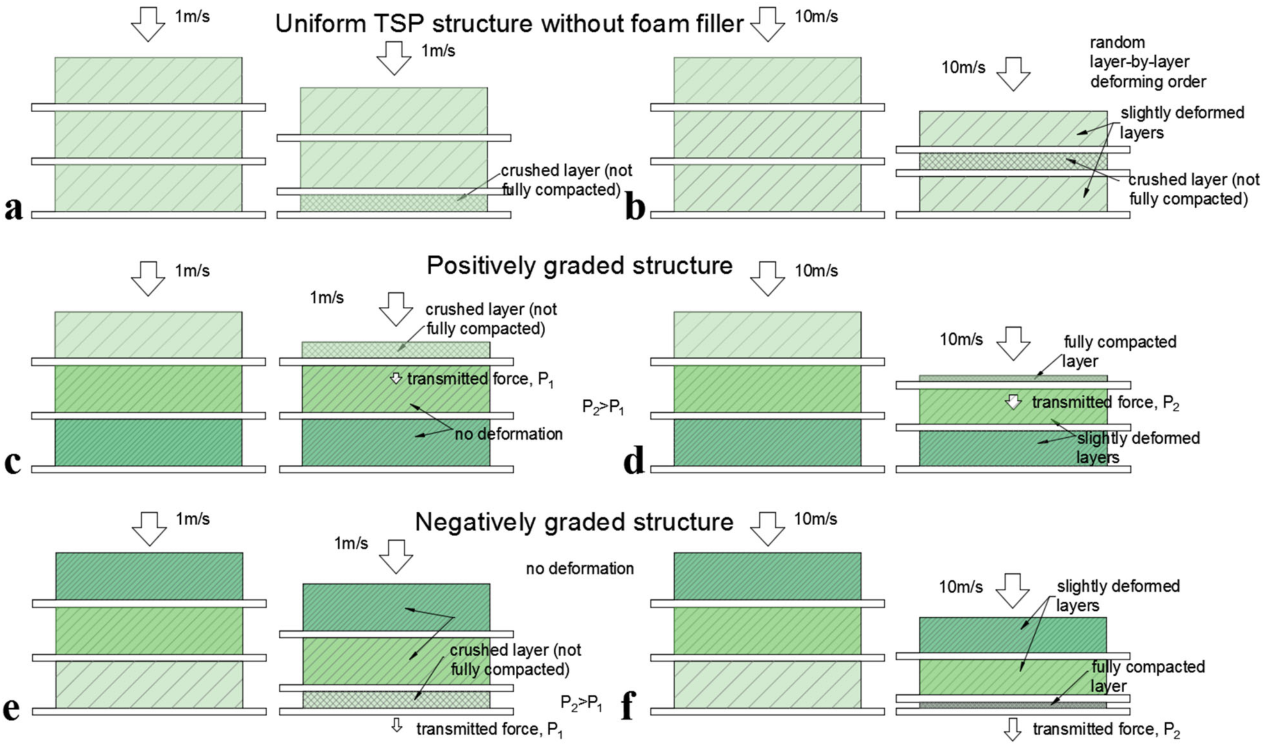

Figure 13. Schematic diagram of layer deformation under different loading and graded conditions; (a) No foam filled TSP folded structure under 1 m/s crushing; (b) No foam filled TSP folded structure under 10 m/s crushing; (c) PG structure under 1 m/s crushing; (d) PG structure under 10 m/s crushing; (e) NG structure under 1 m/s crushing; (f) NG structure under 10 m/s crushing; Note: denser lined layer represents the layer with higher compressive strength

To summarize the layer deformation of graded multi-layer folded structure under three graded configurations and two loading speeds, schematic diagrams are shown in Figure 13. Under low crushing speed, layer-by-layer deformation is observed for both graded configurations. The weakest layer deforms first followed by the second weaker layer. Under 10 m/s crushing, however, slight deformation on all three layers is observed prior to layer-by-layer crushing for both NG and PG structures. Different from that under low crushing speed, the weakest layer is completely crushed under 10 m/s impact before large crushing starts in the next weakest layer. This full compaction of layer may result in a significant increase in force transmitted to the structure behind if the fully crushed layer is the bottom layer. It is also worth noting that the layer-by-layer deforming order for uniform TSP folded structure under 1 m/s impact starts from bottom layer. Random deforming order is observed for 10 m/s impacting case, as the impacting speed is not sufficiently high to cause the failure at impacting end while the interaction of reflected and propogating stress wave is not nessarilly occurs at base end under this impacting speed.

4.2.2 Structural response and energy absorption (10 m/s crushing)

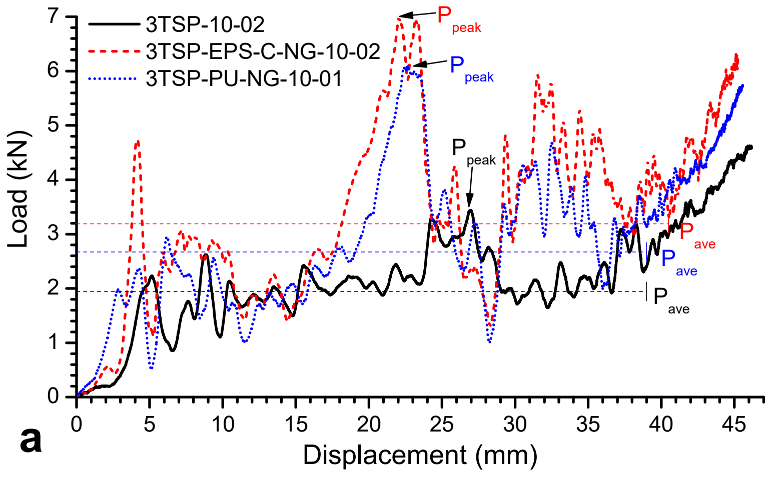

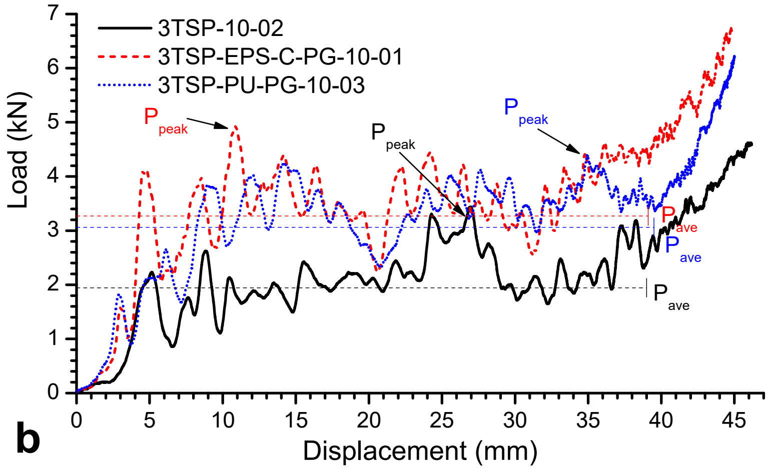

Figure 14. Load-displacement curves of uniform multi-layer TSP folded structure and (a) negatively graded folded structures; (b) positively graded folded structures, under 10 m/s crushing

Load-displacement curves of the multi-layer graded structures under 10 m/s crushing are shown in Figure 14. Crushing responses of these graded folded structures under 10 m/s are very different, as compared to those under low crushing speed of 1 m/s. Fluctuation of the curves can be observed on both the negatively and positively graded cases. For negatively graded folded structures, three sudden rises can be identified on both EPS and PU foam filled NG structures. Out of which, the second peak at around 22 mm of crushed distance shows the highest rise and drop in force as marked out in Figure 14 (a). The peak value at this point is almost twice than the average crushing resistance and almost 40% higher than that of PG counterparts. As previously explained, the collision of the middle and bottom plates as well as full compaction of the weakest layer, which is the bottom layer for NG structures, lead to large force transmitted to the structure behind. For the positively graded folded structure, the load fluctuates around the average line of the crushing force and the fluctuation is much smaller in amplitude, indicating a more uniform crushing response. Clear change in initial stiffness can be observed as well. For the first 2 to 3 mm of the crushing, the stiffness of all structures is much lower than that after initial stage, which is caused by the gap between foldcores and plates. Once the manual folding induced gaps are closed, the crushing stiffness rises quickly, which can be observed for PG and NG cases in Figure 14. The slopes of the initial stage of crushing after gap closing are much higher than those under 1 m/s crushing shown in Figure 9 due to inertia effect and stabilization effect of the cell walls.

Table 4. Crushing responses of different graded structures under 10 m/s crushing speed

Graded configurations	**P_{peak} (kN)**	**P_{ave} (kN)**	**U= P_{peak} /P_{ave}**	**ε_D**	**SEA (J/g)**
3TSP-10-02	3.44	1.94	1.773	0.65	2.70
3TSP-EPS-C-NG-10-02	6.97	3.19	2.206	0.68	4.37
3TSP-PU-NG-10-01	6.10	2.67	2.285	0.65	3.37
3TSP-EPS-C-PG-10-01	4.93	3.27	1.508	0.65	4.32
3TSP-PU-PG-10-03	4.40	3.06	1.438	0.66	3.91

The structural response and energy absorption of the graded structures under 10 m/s are listed in Table 4. The peak crushing forces for two configurations of negatively graded structures (3TSP-EPS-C-NG, 3TSP-PU-NG) are around 40% larger than their positively graded counterparts (3TSP-EPS-C-PG, 3TSP-PU-PG) under 10 m/s loading. On the other hand, the energy absorption and average crushing resistance of these NG structures are similar or lower than their PG counterparts. Both negatively graded structures (3TSP-EPS-C-NG, 3TSP-PU-NG) show less uniform crushing behaviour than the uniform and PG structures, by yielding a larger uniformity ratio. Positively graded structures, however, have smaller uniformity ratios than NG structures and uniform folded structures, demonstrating the improved crushing behaviour by adding positively graded foam fillers, which not only enhance the energy absorption but also lead to a more uniform crushing process.

For the structures with both PU and EPS positively graded foam infill, the specific energy absorption (SEA) is above 4.3 J/g under 10 m/s crushing, which is much superior to the uniform folded structure without foam infill. The energy absorption is also much higher than some conventional energy absorbing material and structures such as aluminium foam and eggbox made of aluminium thin sheet of similar density [7]. Under quasi-static loading, the aluminium eggbox with volumetric density of 2.8% has the SEA around 1 J/g and the Cymat® aluminium foam with 3.1% volumetric density has the SEA between 0.5 and 0.8 J/g [7, 27].

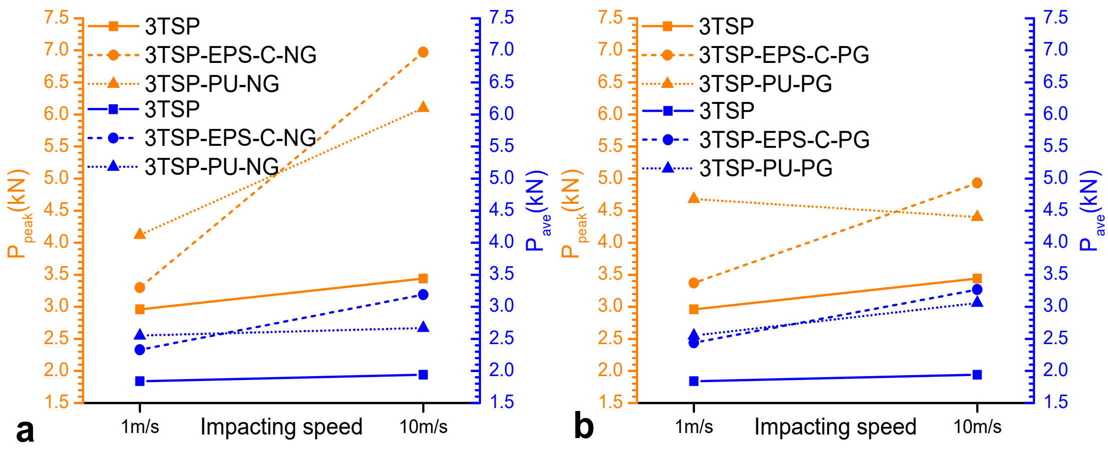

Figure 15. Peak and average crushing forces with the increase of impacting speed for (a) negatively graded structures; (b) positively graded structures

Figure 15 shows the comparison of the peak and average crushing forces among the folded graded structures under low and high crushing speeds. With the increasing crushing speed, rises in average crushing forces can be observed for all graded configurations and the uniform foldcore without foam fillers. This is due to the structural stabilization and change of damage mode on some layers with the increasing crushing speed. With the increase of impacting speed from 1m/s to 10 m/s, the changes of the peak crushing forces are different for the two graded (PG/NG) configurations. As shown in Figure 15 (a), much higher rise of peak crushing force is shown for the negatively graded (NG) structure due to the quick full compaction of the bottom layer and impacting onto the base support where the load cell is located. However, for the positively graded structure, the peak force increases slightly or even decreases (e.g. 3TSP-PU-PG as shown in Figure 15 b) when crushing speed increases from 1 to 10 m/s. Under 10 m/s impacting speed, all layers deform slightly before layer-by-layer deformation occurs, as shown in Figure 10. This will increase the initial peak force at early stage due to initiation of buckling on all layers, while the peak at later stage of the crushing is reduced as the layers are slightly buckled prior to layer-by-layer deformation.

Under 10 m/s crushing, the overall peak force occurs at early stage of the deformation for EPS foam filled PG structure (Figure 14 b), different from low speed crushing where the peak force occurs at later stage of deformation (Figure 9 b). For PU foam filled PG structure, overall peak force occurs at later stage of the deformation under both crushing speeds. For both PG structures (EPS and PU), the deforming orders are the same, from top to bottom layer under both crushing speeds, whereas slight deformation occurs on all three layers before layer-by-layer deformation under higher crushing speed. This leads to the increase in crushing force at early stage and reduction at later stage under higher crushing speed, as explained in the previous paragraph. Illustration of this change in crushing force at early and later stages under 1 and 10 m/s crushing is shown in Figure 16. It is worth noting that the illustration only shows the changes caused by the slight simultaneous buckling on all three layers before layer-by-layer crushing under 10 m/s loading, it does not include other factors such as inertia effect and stabilization of the foam which result in a higher average crushing force under higher crushing speed as previously explained. For EPS foam filled PG structure, the difference in compressive strength from top to bottom layers (EPS 13.5, EPS19, EPS 28) is not significant. Therefore, with the increasing loading rate from 1 to 10 m/s, the appearance of peak force changes from later stage P_2 (10 m/s) to early stage P_1 (10 m/s) due to the increase of crushing force at early stage as shown in Figure 16 (a). For PU foam filled PG structure, the compressive strength from top to bottom layers is very different due to foam filler configuration (no foam, cubic foam and shaped foam from top to bottom layer). Therefore, under 10 m/s crushing, even with the increase in crushing force at early stage and decrease at later stage, the crushing force at early stage P_1 (10 m/s) is still smaller than that at later stage P_2 (10 m/s) where bottom layer with shaped foam is being crushed as shown in Figure 16 (b). Therefore, overall peak crushing force of PU foam filled PG structure occurs at later stage and its value is slightly reduced comparing to 1 m/s crushing case.

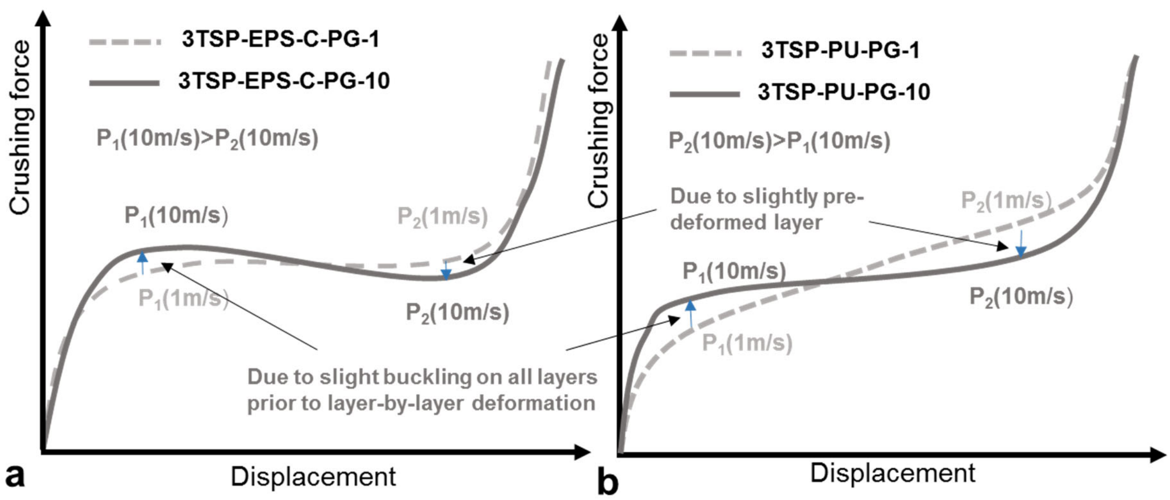

Figure 16. Illustration of changes in peak forces at early and later stage of crushing under 1 and 10 m/s impact for (a) EPS foam filled PG structure; (b) PU foam filled PG structure; note: this graph is only used to illustrate the changes in peak forces caused by the change of layer deformation mode under 1 and 10 m/s impact, does not represent the actual crushing responses

5 Conclusions

Two sets of negatively and positively graded TSP folded structures by varying foam filler configurations are experimentally studied. Their crushing behaviours including peak and average crushing force, energy absorption, uniformity ratio and damage modes are compared under two different speeds. It is found that the structures with different graded configurations show similar crushing behaviors under low crushing speeds, indicating the graded configurations have minimum influences on the impact responses of the graded TSP folded structures. Under high crushing speed, however, significant advantages are obtained for positively graded structure where the core strength increases along the impacting direction. More uniform load-displacement responses with lower fluctuation, lower peak force and higher energy absorption are achieved for positively graded structures with two sets of foam filler configurations than their negatively graded counterparts. Different damage modes are observed for these graded structures as well. Layer-by-layer crushing with initiation on the weakest layer is observed on graded structure under low crushing rate. Under high crushing speed, all three layers undergo a slight simultaneous deformation prior to the layer-by-layer crushing. Due to foam-shell interaction effect, an excellent graded performance can be achieved by inserting lightweight foam, which leads to an up to 68.6% increase in average crushing force with only a 5.3% increase in structural mass. Furthermore, the graded configuration of this multi-layer TSP folded structure can be easily modified according to various scenarios by relocating the desired foam filler, as no permanent bonding between foldcores and plates is required. The interlayer plates of the set-up are also reusable, the core can be easily replaced after each use. Overall, with suitable graded configuration, this graded multi-layer TSP folded structure has superior energy absorption capacity than uniform TSP folded structure especially under dynamic loading conditions.

Acknowledgements

The authors acknowledge the support from Australian Research Council via Discovery Early Career Researcher Award (DE160101116). The authors acknowledge the assistance provided by Ms. Xiaochen Yang from Motion Structure Laboratory in Tianjin University for 3D Direct Image Correlation analysis of the foldcores and Ms. Samantha Tyson from Curtin University for testing preparations.

References

[1] Lu G, Yu T. Energy Absorption of Structures and Materials. Cambridge England: Woodhead publishing limited; 2003.

[2] Gibson LJ, Ashby MF. Cellular solids: structure and properties: Cambridge university press; 1999.

[3] Sun G, Chen D, Wang H, Hazell PJ, Li Q. High-velocity impact behaviour of aluminium honeycomb sandwich panels with different structural configurations. International Journal of Impact Engineering. 2018;122:119-36.

[4] Nieh T, Higashi K, Wadsworth J. Effect of cell morphology on the compressive properties of open-cell aluminum foams. Materials Science and Engineering: A. 2000;283(1):105-10.

[5] Jiang B, Wang Z, Zhao N. Effect of pore size and relative density on the mechanical properties of open cell aluminum foams. Scripta Materialia. 2007;56(2):169-72.

[6] Ouellet S, Cronin D, Worswick M. Compressive response of polymeric foams under quasi-static, medium and high strain rate conditions. Polymer Testing. 2006;25(6):731-43.

[7] Zupan M, Chen C, Fleck NA. The plastic collapse and energy absorption capacity of egg-box panels. International Journal of Mechanical Sciences. 2003;45(5):851-71.

[8] Haldar A, Guan ZW, Cantwell WJ, Wang QY. The compressive properties of sandwich structures based on an egg-box core design. Composites Part B: Engineering. 2018;144:143-52.

[9] Wang Z, Liu J, Hui D. Mechanical behaviors of inclined cell honeycomb structure subjected to compression. Composites Part B: Engineering. 2017;110:307-14.

[10] Ozdemir Z, Hernandez-Nava E, Tyas A, Warren JA, Fay SD, Goodall R, et al. Energy absorption in lattice structures in dynamics: Experiments. International Journal of Impact Engineering. 2016;89:49-61.

[11] Cao BT, Hou B, Zhao H, Li YL, Liu JG. On the influence of the property gradient on the impact behavior of graded multilayer sandwich with corrugated cores. International Journal of Impact Engineering. 2018;113:98-105.

[12] Liu T, Hou S, Nguyen X, Han X. Energy absorption characteristics of sandwich structures with composite sheets and bio coconut core. Composites Part B: Engineering. 2017;114:328-38.

[13] Li Z, Chen W, Hao H. Numerical study of sandwich panel with a new bi-directional Load-Self-Cancelling (LSC) core under blast loading. Thin-Walled Structures. 2018;127:90-101.

[14] Xue Z, Hutchinson JW. Crush dynamics of square honeycomb sandwich cores. International Journal for Numerical Methods in Engineering. 2006;65(13):2221-45.

[15] Kılıçaslan C, Güden M, Odacı İK, Taşdemirci A. Experimental and numerical studies on the quasi-static and dynamic crushing responses of multi-layer trapezoidal aluminum corrugated sandwiches. Thin-Walled Structures. 2014;78:70-8.

[16] Wang Z, Liu J, Lu Z, Hui D. Mechanical behavior of composited structure filled with tandem honeycombs. Composites Part B: Engineering. 2017;114:128-38.

[17] Mohsenizadeh M, Gasbarri F, Munther M, Beheshti A, Davami K. Additively-manufactured lightweight Metamaterials for energy absorption. Materials & Design. 2018;139:521-30.

[18] Zhu F, Lu G, Ruan D, Wang Z. Plastic deformation, failure and energy absorption of sandwich structures with metallic cellular cores. International Journal of Protective structures. 2010;1(4):507-41.

[19] Deshpande VS, Ashby MF, Fleck NA. Foam topology bending versus stretching dominated architectures. Acta Materialia. 2001;49(6):1035-40.

[20] Heimbs S. Foldcore sandwich structures and their impact behaviour: an overview. Dynamic failure of composite and sandwich structures: Springer; 2013. p. 491-544.

[21] Karagiozova D, Zhang J, Lu G, You Z. Dynamic in-plane compression of Miura-ori patterned metamaterials. International Journal of Impact Engineering. 2019.

[22] Herrmann AS, Zahlen PC, Zuardy I. Sandwich structures technology in commercial aviation. Sandwich structures 7: Advancing with sandwich structures and materials: Springer; 2005. p. 13-26.

[23] Zhou C, Wang B, Ma J, You Z. Dynamic axial crushing of origami crash boxes. International Journal of Mechanical Sciences. 2016;118:1-12.

[24] Gattas JM, You Z. The behaviour of curved-crease foldcores under low-velocity impact loads. International Journal of Solids and Structures. 2015;53:80-91.

[25] Fang H, Chu SA, Xia Y, Wang KW. Programmable Self-Locking Origami Mechanical Metamaterials. Adv Mater. 2018;30(15):e1706311.

[26] Li Z, Chen W, Hao H. Crushing behaviours of folded kirigami structure with square dome shape. International Journal of Impact Engineering. 2018;115:94-105.

[27] Li Z, Chen W, Hao H, Cui J, Shi Y. Experimental study of multi-layer folded truncated structures under dynamic crushing. International Journal of Impact Engineering. 2019;131:111-22.

[28] Li Z, Chen W, Hao H. Dynamic crushing and energy absorption of foam filled multi-layer folded structures: Experimental and numerical study. International Journal of Impact Engineering. 2019;133:103341.

[29] Li G, Xu F, Sun G, Li Q. A comparative study on thin-walled structures with functionally graded thickness (FGT) and tapered tubes withstanding oblique impact loading. International Journal of Impact Engineering. 2015;77:68-83.

[30] Zhang H, Sun G, Xiao Z, Li G, Li Q. Bending characteristics of top-hat structures through tailor rolled blank (TRB) process. Thin-Walled Structures. 2018;123:420-40.

[31] Sun G, Li G, Hou S, Zhou S, Li W, Li Q. Crashworthiness design for functionally graded foam-filled thin-walled structures. Materials Science and Engineering: A. 2010;527(7-8):1911-9.

[32] Sun G, Wang E, Wang H, Xiao Z, Li Q. Low-velocity impact behaviour of sandwich panels with homogeneous and stepwise graded foam cores. Materials & Design. 2018;160:1117-36.

[33] Zhang L, Hebert R, Wright JT, Shukla A, Kim J-H. Dynamic response of corrugated sandwich steel plates with graded cores. International Journal of Impact Engineering. 2014;65:185-94.

[34] Li S, Wang Z, Wu G, Zhao L, Li X. Dynamic response of sandwich spherical shell with graded metallic foam cores subjected to blast loading. Composites Part A: Applied Science and Manufacturing. 2014;56:262-71.

[35] Shen CJ, Lu G, Yu TX. Dynamic behavior of graded honeycombs – A finite element study. Composite Structures. 2013;98:282-93.

[36] Gardner N, Wang E, Shukla A. Performance of functionally graded sandwich composite beams under shock wave loading. Composite Structures. 2012;94(5):1755-70.

[37] Ma J, Song J, Chen Y. An origami-inspired structure with graded stiffness. International Journal of Mechanical Sciences. 2018;136:134-42.

[38] Maskery I, Hussey A, Panesar A, Aremu A, Tuck C, Ashcroft I, et al. An investigation into reinforced and functionally graded lattice structures. Journal of Cellular Plastics. 2016.

[39] Xiao L, Song W. Additively-manufactured functionally graded Ti-6Al-4V lattice structures with high strength under static and dynamic loading: Experiments. International Journal of Impact Engineering. 2017.

[40] Gattas JM, You Z. Quasi-static impact of indented foldcores. International Journal of Impact Engineering. 2014;73:15-29.

[41] Avallone E, Baumeister T. Mark's standard handbook for mechanical engineers: McGraw-Hill; 2017.

[42] Li Z, Chen W, Hao H. Blast mitigation performance of cladding using Square Dome-shape Kirigami folded structure as core. International Journal of Mechanical Sciences. 2018;145:83-95.

[43] ASTM. B209M-14: Standard Specification for Aluminum and Aluminum-Alloy Sheet and Plate (Metric). ASTM International West Conshohocken; 2014.

[44] Chen W, Hao H, Hughes D, Shi Y, Cui J, Li Z-X. Static and dynamic mechanical properties of expanded polystyrene. Materials & Design. 2015;69:170-80.

[45] Yu T, Qiu X. Introduction to impact dynamics: John Wiley & Sons; 2018.

[46] Pham TM, Chen W, Kingston J, Hao H. Impact response and energy absorption of single phase syntactic foam. Composites Part B: Engineering. 2018;150:226-33.

[47] Pham TM, Chen W, Hao H. Failure and impact resistance analysis of plain and fiber-reinforced-polymer confined concrete cylinders under axial impact loads. International Journal of Protective Structures. 2018;9(1):4-23.

[48] Chen W, Wierzbicki T. Relative merits of single-cell, multi-cell and foam-filled thin-walled structures in energy absorption. Thin-Walled Structures. 2001;39(4):287-306.

[49] Sun G, Li S, Liu Q, Li G, Li Q. Experimental study on crashworthiness of empty/aluminum foam/honeycomb-filled CFRP tubes. Composite Structures. 2016;152:969-93.

[50] Wang Z, Liu J. Mechanical performance of honeycomb filled with circular CFRP tubes. Composites Part B: Engineering. 2018;135:232-41.

[51] Ousji H, Belkassem B, Louar MA, Reymen B, Martino J, Lecompte D, et al. Air-blast response of sacrificial cladding using low density foams: Experimental and analytical approach. International Journal of Mechanical Sciences. 2017;128-129:459-74.

[52] Ma GW, Ye ZQ. Analysis of foam claddings for blast alleviation. International Journal of Impact Engineering. 2005;34(1):60-70.